Electronic Supplementary Material (ESI) for Materials Advances.

Enabling Fine-Grain Free 2 Micron Thick CISe/CIGSe Film Fabrication From A Non-Hydrazine Based Solution Processing Route

Swapnil D. Deshmukh,[1] Kyle G. Weideman,[1] Ryan G. Ellis,[1] Kim Kisslinger,[2] Rakesh Agrawal[1]*

[1]Davidson School of Chemical Engineering, Purdue University, West Lafayette, IN 47907, USA

[2]Center for Functional Nanomaterials, Brookhaven National Laboratory, Upton, NY 11973, USA

Supporting Information

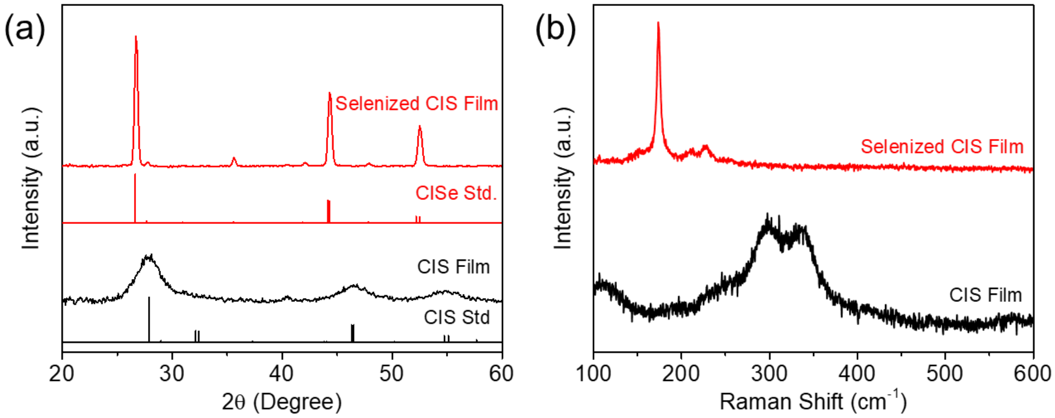

Figure S1. (a) XRD and (b) Raman spectra of precursor CIS film and selenized film confirming the formation of phase pure chalcopyrite $CuInSe_2$ material (CIS XRD Std- ICSD collection #186714, CISe XRD Std- ICSD collection #73351)

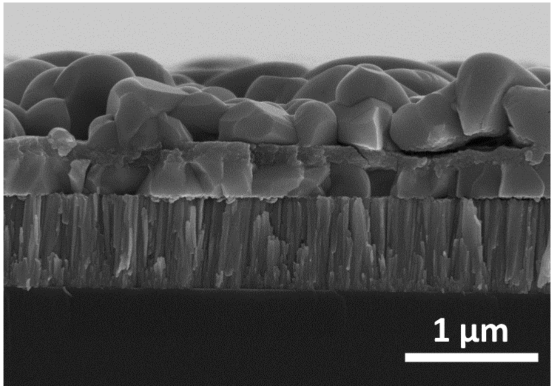

Figure S2. Cross-section SEM image of selenized CIGS film showing formation of trilayer morphology similar to the one observed for selenized CIS film

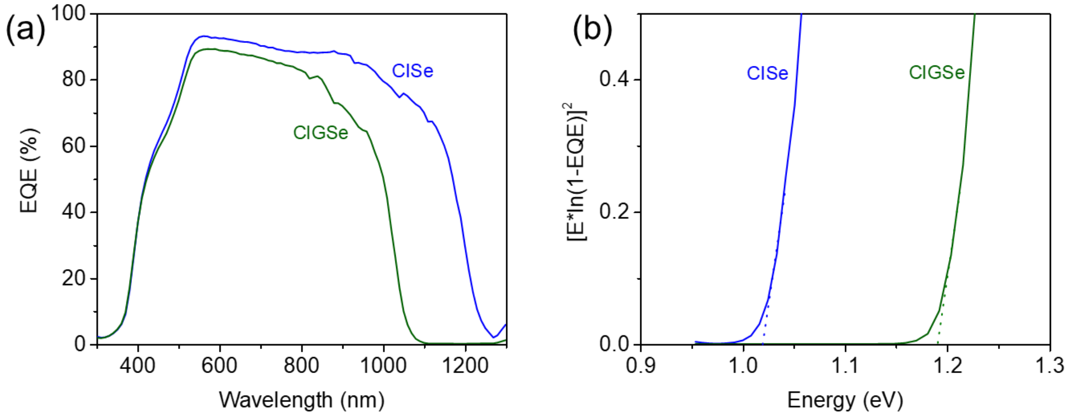

Figure S3. (a) EQE and (b) bandgap extrapolation from EQE for highest efficiency CISe and CIGSe films

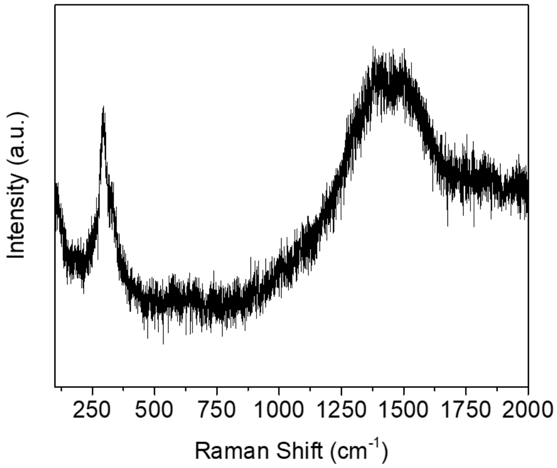

Figure S4. Raman spectrum of precursor CIS film showing presence of strong graphitic carbon peak in the range of 1300-1600 cm^{-1}

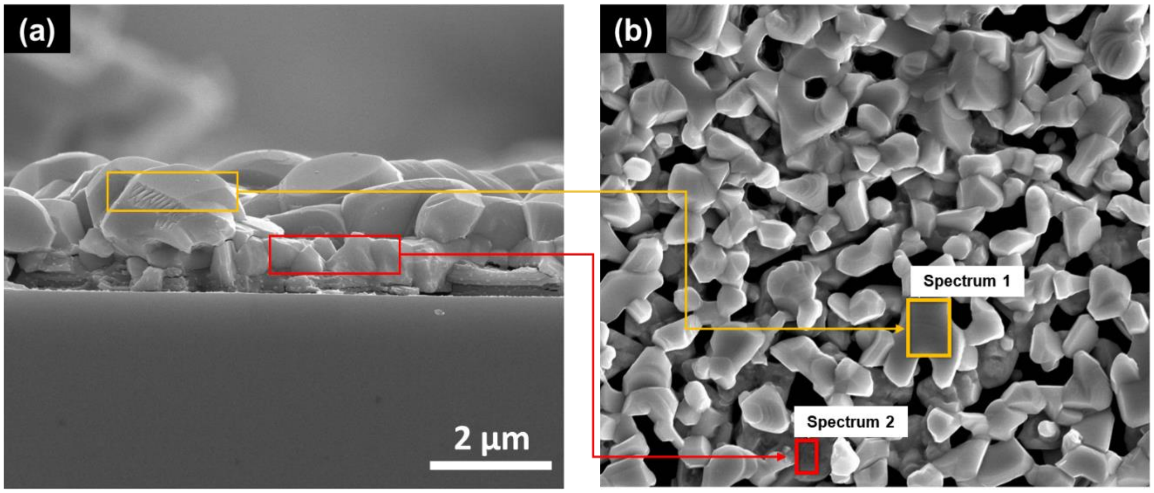

		Cu	In	Se	S	Cu/In	Se/(Cu+In)
Top Grain	Spectrum 1	14.7	14.5	27.76	1.05	1.01	0.95
Bottom Grain	Spectrum 2	15.36	20.08	30.04	1.93	0.76	0.84

Figure S5. (a) Cross-section and (b) top view SEM images of 2 µm thick selenized CIS film fabricated from DMF-TU route showing two different grain compositions for top and bottom grain layer collected using SEM-EDS

Se Addition in Precursor Film

Se addition to the sulfide ink was performed to get Se/In ratio of 1, 2, and 4 corresponding to 50% of stoichiometric, stoichiometric, and 100% excess Se respectively. Precursor films fabricated from these inks after coating and annealing on hot plate resulted in the formation of sulfoselenide material which was analyzed using Raman spectroscopy and X-ray fluorescence (XRF). All films showed peaks corresponding to both CIS and CISe material with higher Se containing inks showing a higher relative ratio of the CISe/CIS peak in the Raman spectra (Figure S6). Similarly, XRF showed a Se/In ratio of 0.5, 1.4, and 1.8 for the films fabricated from inks having Se/In ratio of 1, 2, and 4 respectively. The 100% excess Se ink appeared to give mostly selenide material, however, due to the use of the excess quantity of elemental Se in the ink, the precursor film exhibited porous morphology caused by loss of volume via free selenium evaporation during the annealing process (Figure S7).

Such porous precursor films cannot be used for creating a dense absorber layer as it would lead to a possible shunting in the device. While one could dilute the ink to minimize this porosity, using such a dilute ink will require an excessive number of coatings for creating the desired thickness of the film posing difficulty for scale-up. Also, despite using 100% excess Se in the ink (Se/In ratio of 4), the final Se/In ratio in the film was only 1.8 which suggests most of the Se is lost via vaporization during annealing and doesn’t get incorporated in the film.

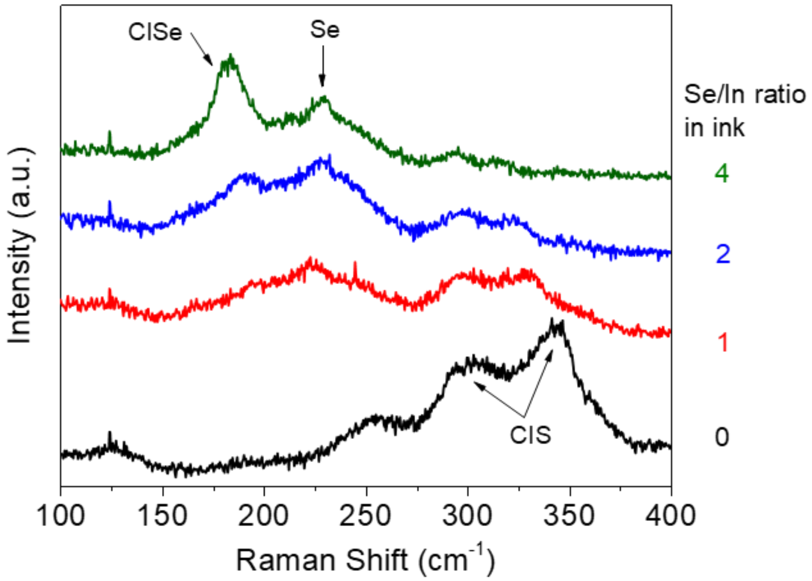

Figure S6. Raman spectra of CISSe precursor films fabricated using CIS precursor ink with addition of different quantities of free Se in the ink

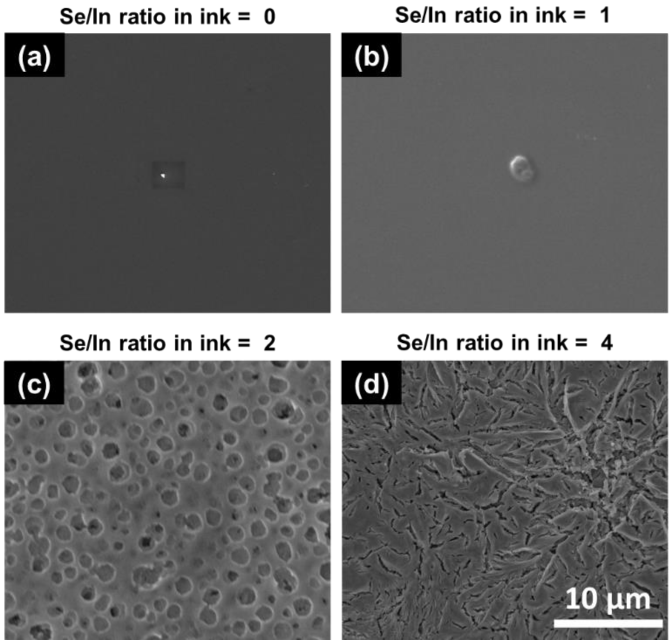

Figure S7. Top-view SEM images of precursor films fabricated using CIS inks containing different Se quantities. (a) 0%, (b) 50% of stoichiometric, (c) stoichiometric, and (d) 100% excess

Another possible route for incorporating Se in the precursor film could be a two-step process where CIS is formed first and then it reacts with elemental Se in the film giving CISe material. In such a process, due to the formation of CIS material in the first step, the carbon content will remain higher. This possible mechanism was confirmed when films were fabricated from an ink having Se/In ratio of 2 at different temperatures. The sudden exposure to higher temperature allowed for quick decomposition of thiolates to sulfides along with rapid evaporation of free Se from the film giving more CIS material and carbon compared to film annealed at a lower temperature which has more Se incorporation and less carbon (Figure S8).

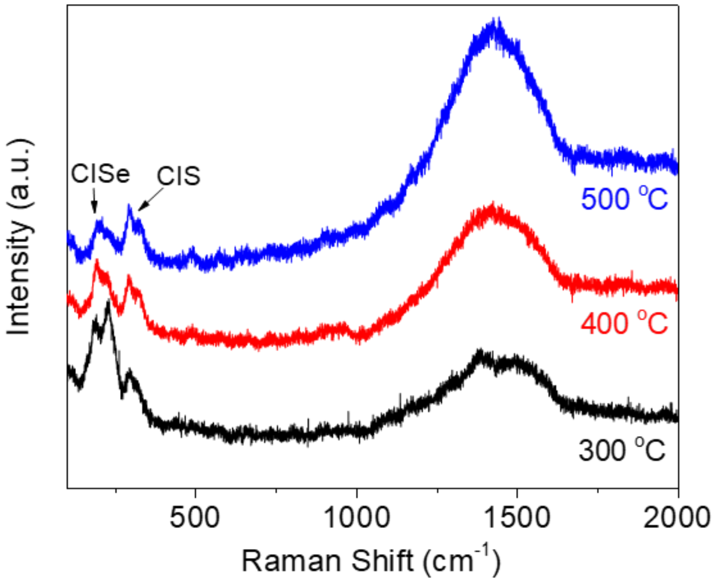

Figure S8. Raman spectra of precursor films coated with Cu_2S+In+Se+BA+EDT solution containing Se/In of 2 and annealed at different temperatures immediately after coating showing increasing CIS/CISe peak ratio and carbon peak intensity with increasing temperature

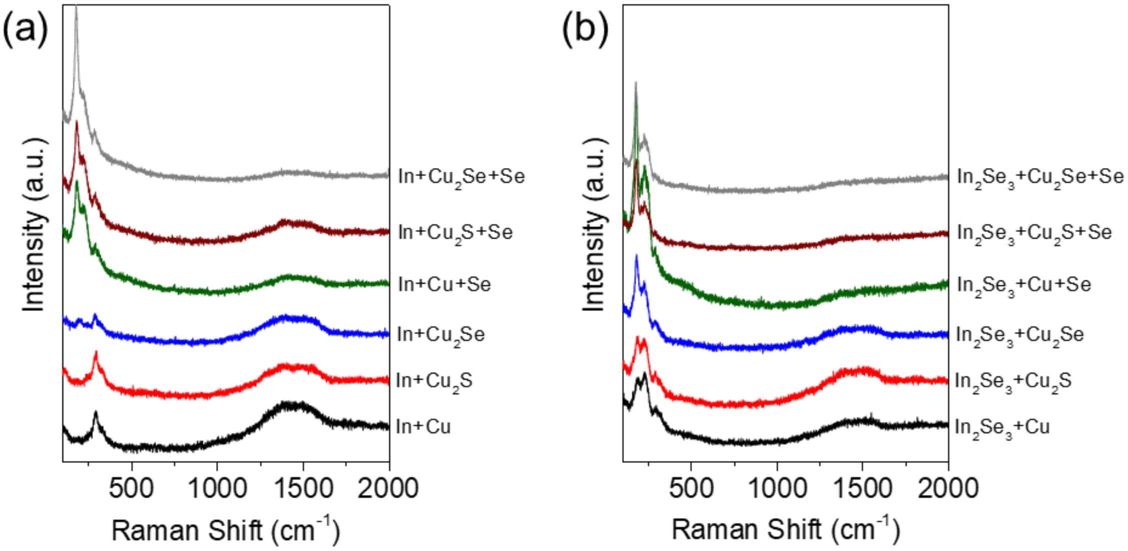

Figure S9. Raman spectra of films annealed at 300 °C and coated from inks containing (a) In metal along with different Cu and Se precursors and (b) In_2Se_3 along with different Cu and Se precursors showing reduction in carbon peak (1300-1600 cm^{-1}) when In is replaced with In_2Se_3 and also with addition of free Se. All inks with free Se contains free Se to In ratio of 2

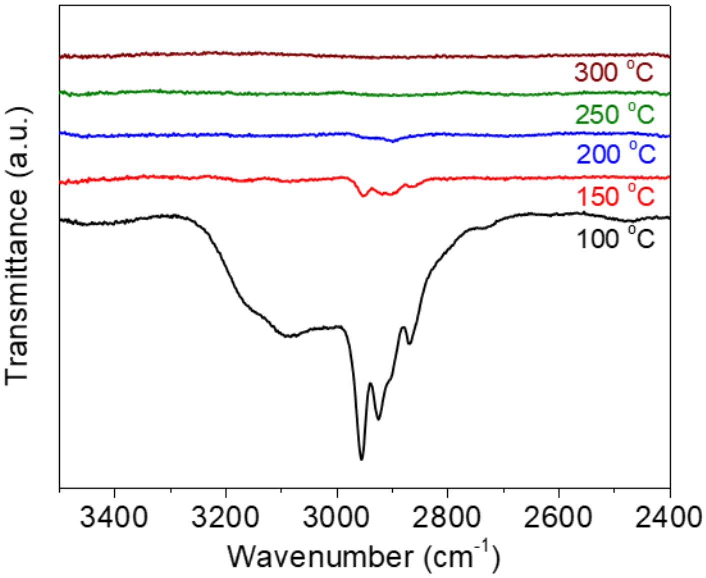

Figure S10. FTIR spectra collected on films coated using Cu_2Se+In_2Se_3+Se+BA+EDT (total Se/In = 4) solution annealed at different temperatures showing removal of organic carbon residue at temperature as low as 250 °C

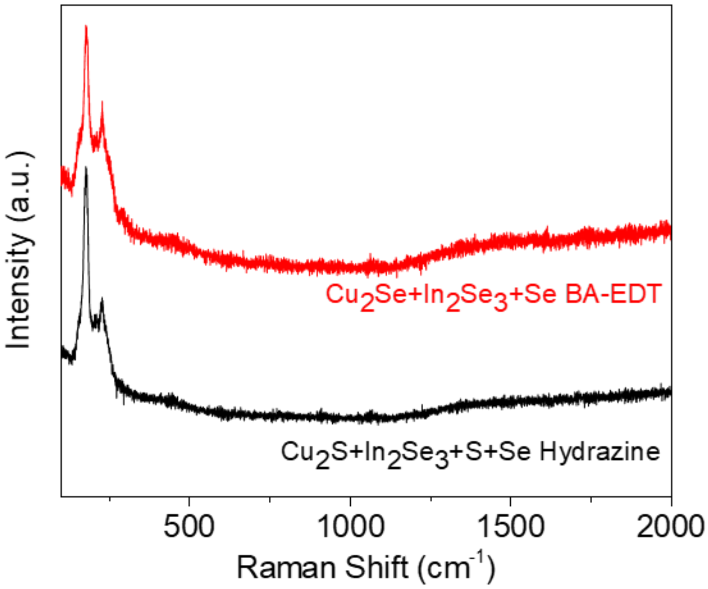

Figure S11. Raman spectra of precursor CISe films fabricated from BA-EDT solution and hydrazine solution showing similar Raman response in both the films

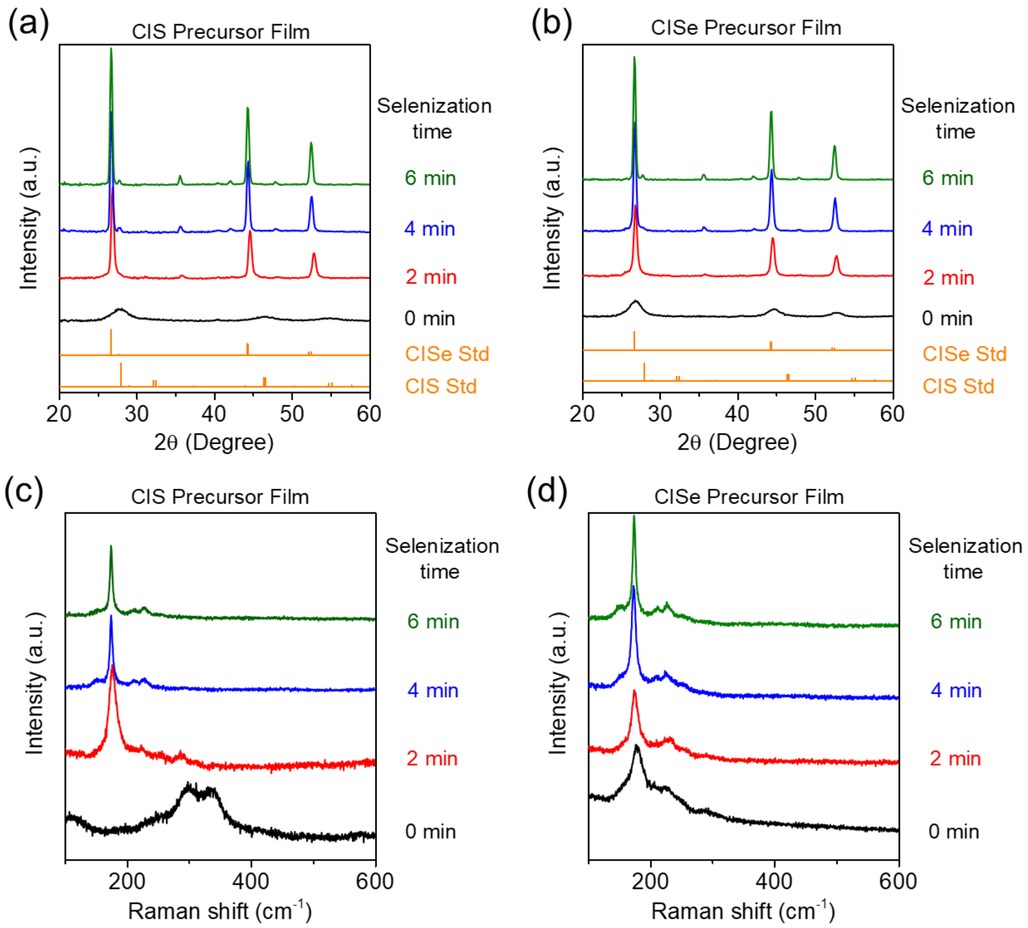

Figure S12. (a,b) XRD spectra and (c,d) Raman spectra of CIS and CISe films respectively selenized for different time intervals (CIS XRD Std- ICSD collection #186714, CISe XRD Std- ICSD collection #73351)

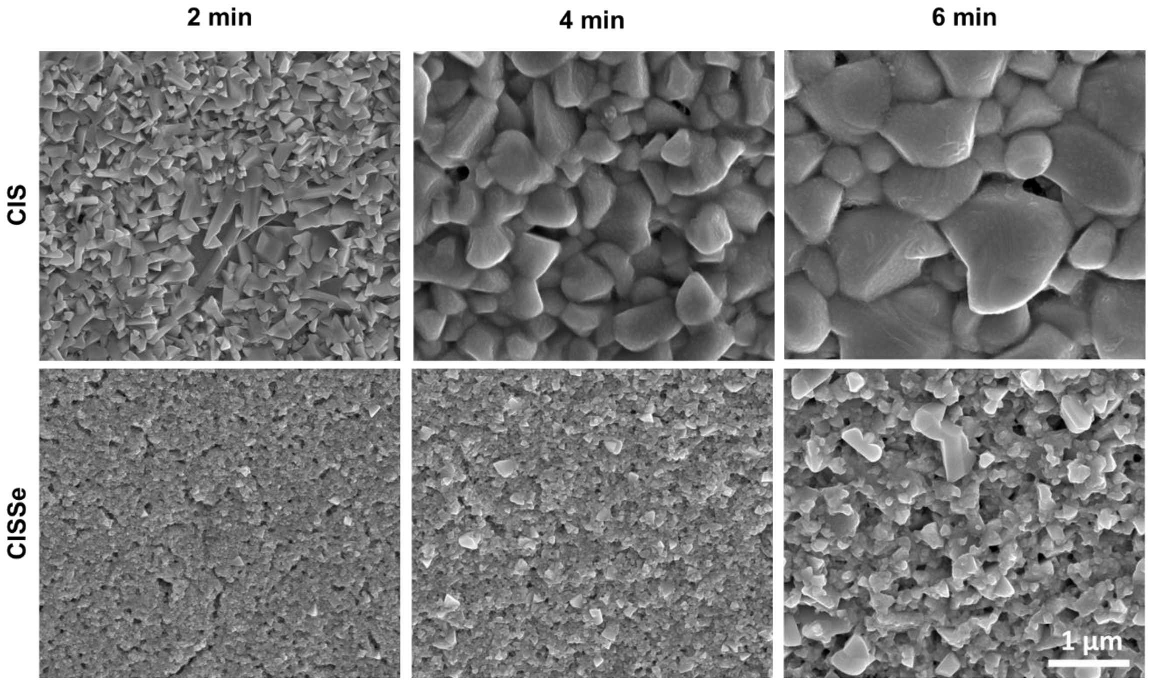

Figure S13. Top view SEM images of selenized CIS and CISe precursor films for different time intervals

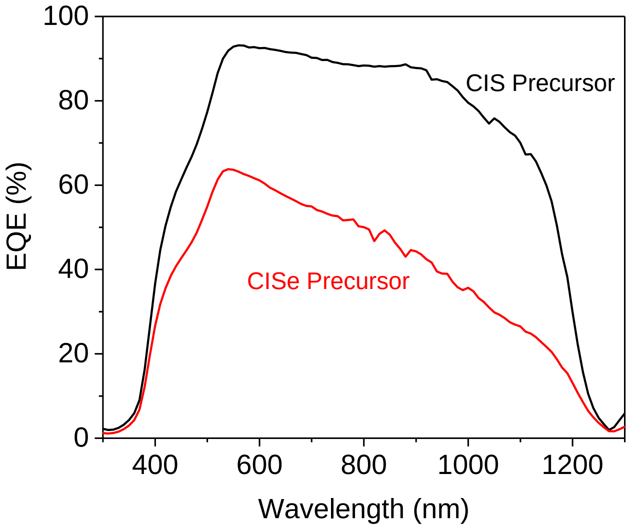

Figure S14. EQE data on CISe devices fabricated from CISe precursor film and CIS precursor film showing poor current collection for the device from CISe precursor film

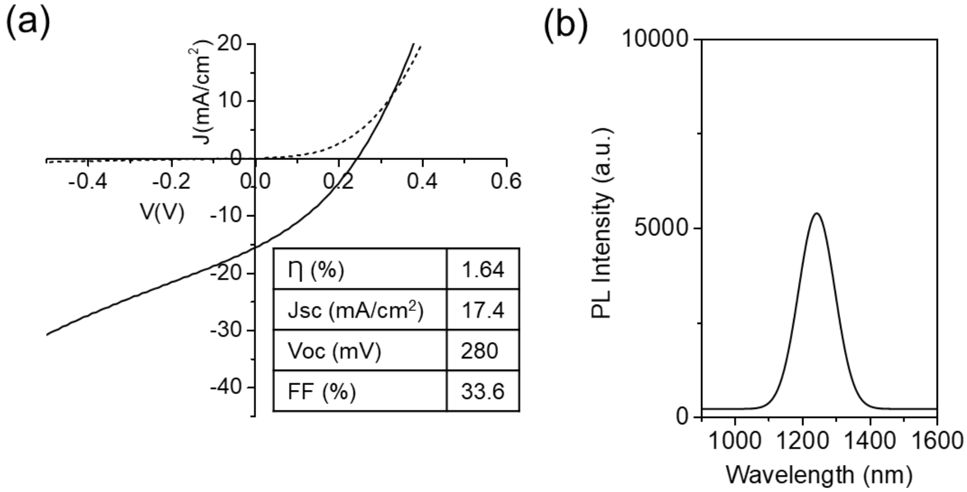

η (%)	1.64
Jsc (mA/cm^2)	17.4
Voc (mV)	280
FF (%)	33.6

Figure S15. (a) JV data and (b) PL spectrum of CISe film fabricated from hydrazine route showing poor power conversion efficiency and also an order of magnitude lower PL intensity compared to device fabricated from amine-thiol-CIS precursor film

Scheme S1. Proposed mechanism of metal thiolate decomposition in (a) absence and (b) presence of Se anion